Hindawi
Journal of Nanomaterials
Volume 2017, Article ID 7601869, 11 pages
https://doi.org/10.1155/2017/7601869

Research Article

Structural Derivative and Electronic Property of Armchair Carbon Nanotubes from Carbon Clusters

Yuchao Tang,[1] Junzhe Lu,[2] Denghui Liu,[1] Xuejun Yan,[1] Chengpeng Yao,[1] and Hengjiang Zhu[1,2]

[1] *College of Physics and Electronic Engineering, Xinjiang Normal University, Urumqi 830054, China*
[2] *Key Laboratory of Mineral Luminescence Materials and Microstructures of Xinjiang Uygur Autonomous Region, Urumqi 830054, China*

Correspondence should be addressed to Hengjiang Zhu; zhj@xjnu.edu.cn

Received 16 September 2016; Accepted 14 November 2016; Published 8 February 2017

Academic Editor: Yu-Lun Chueh

The structural derivative and electronic property of carbon nanotubes from carbon clusters were investigated by density functional theory (DFT), including armchair single-walled carbon nanotubes (SWCNTs) and multiwalled carbon nanotubes (MWCNTs). Results show that the carbon nanotubes (CNTs) can be obtained through layer-by-layer growth from the initial structure. The structural derivative processes are quantitatively described by monitoring changes in local configuration. Electronic properties show the energy gaps of finite SWCNTs and double-walled CNTs (DWCNTs) depending on their lengths. However, the band structures of MWCNTs differ from those of SWCNTs; the band structures of DWCNTs (4, 4)@(8, 8), (5, 5)@(10, 10), and TWCNTs show metallicity, whereas those of (3, 3)@(6, 6) DWCNTs show a strong semiconductor characteristic. Analysis of the partial density of states shows that the diameters and walls of CNTs have no obvious effects on the distribution of total density of states near the Fermi level of SWCNTs and MWCNTs.

1. Introduction

Recently, the emerging need for ultra-high-speed electronics and renewable energy has motivated the investigation and development of new classes of nanomaterials in unconventional device fields [1]. Among these materials, carbon nanomaterials have gained extraordinary attention due to their unique structures and excellent properties [2]. Interest in CNTs continues to grow since their discovery by Iijima [3]. CNTs have gained great attention due to its unique physical properties (elasticity, low density, deformation, high stiffness and strength, and excellent electric properties) and various technological applications (semiconducting, H_2 storage, and probes) [4–11]. CNTs are synthesized via carbon-arc discharge [12, 13], laser vaporization [14, 15], catalytic combustion [16, 17], and chemical vapor deposition (CVD) [18]. Although there are many ways to produce CNTs, the current techniques for the preparation of CNTs are far from meeting these practical requirements. Therefore, it is essential to understand the growth process from atomic-level for the preparation of CNTs.

At present, due to the restrictions of detection and analysis measurements, it is difficult to study the growth process of CNTs in experiments. So far, there has been little theoretical information about the CNTs growth process. The growth process of CNTs is studied mainly by two approaches; one is to conceptualize a possible growth process according to the structural characters of CNTs obtained from the experiments [19, 20]; and the other is to simulate the growth process via microscopy by MD or QM/MD methods [21, 22]. In 1992, Iijima et al. presented the open-end growth model for carbon nanotubes [23]. In the same year, Nardelli et al. [24] investigated the lip-lip interactions in the growth of DWCNTs. Furthermore, Jin et al. [25] experimentally observed the lip-lip interaction between adjacent concentric shells. Their results showed that lip-lip interaction can effectually steady the open edges and facilitate the growth of DWCNTs. Recently, Kiang [26] and Lin et al. [27] presented a growth model of

Table 1: Bond lengths, bond angles, total energies, and vibration frequencies of the small carbon clusters.

Cluster	Point group	Bond length (Å)	Bond angle (degrees)	Total energy (hartrees)	Vibration frequencies (cm^{-1})
C_2	$D_{\infty h}$	1.252		−75.462	1857.2
		1.259[a]		−75.722[d]	1845[a]
		1.243[b]		−75.379[d]	1855.7[b]
C_4	D_{2h}	1.489	63.7	−151.155	
		1.425[d]	61.5[d]	−151.146[d]	
C_6	D_{3h}	1.313	101.4	−225.477	
		1.313[e]	101.4[e]	−225.477[e]	
		1.316[d]	90.4[d]	−226.803[d]	
C_8	C_{4h}	1.247, 1.399	116.8	−302.691	
		1.26, 1.376[c]	112.6[c]	−302.476[d]	

[a]Theoretical data by B8P6/[4s3p1d] [36]. [b]Experimental data [37]. [c]Theoretical data by B3LYP/cc-pVDZ [38]. [d]Theoretical data by MP4/6-31G* [39]. [e]Theoretical data by HF/3-21G [40].

carbon rings and cages for SWCNTs based on experimental observations and energetic considerations. Later, Raty et al. [28] reported the early stages of SWCNT growth on metal nanoparticles by ab initio molecular dynamic simulations. Their results demonstrate that the initial structure (so-called nucleus) should be formed in early CNTs growth. However, to clearly observe the structures and morphologies of CNTs nuclei (carbon clusters) were difficult. Moreover, theoretical studies of structural derivative process of armchair CNTs from the carbon clusters are lacking, specifically the MWCNTs. In this work, the structural derivative processes of the SWCNTs and MWCNTs were investigated from carbon clusters via bottom-up approach. In the derivative processes, the geometry structures, stability, and electronic properties of SWCNTs and MWCNTs were calculated, which provided a possible guideline for the growth process of armchair CNTs.

2. Computational Methods

In this work, all calculations were performed using the DFT in the GAUSSIAN 03 package [29]. The hybrid density functional B3LYP [30, 31] were then employed to describe the exchange-correlation potential. To better describe the structural features and electronic properties of finite CNTs, the all electron 3-21G(d) basis set, which was used to describe accurately the structures of armchair CNTs in experiment previously [32, 33], has been chosen. Using a higher basis set is expected to enhance the accuracy of calculation of the electronic properties; however, such accuracy has been reported to not generally affect the simulation trends and yet consumes more computational power [34]. In the calculated process, the geometry structures were fully optimized without any symmetrical constraints. The convergence criterion of 10^{-6} a.u. on the total energy was used in geometrical optimizations.

Based on the derivative process of finite CNTs, a basic building block of the infinite SWCNTs and MWCNTs was chosen as a unit cell that was built by removing two parallel polygons at both ends of corresponding finite CNTs. All of the unit cells of the infinite SWCNTs and MWCNTs contain four layers of carbon atoms along the tube axis (taken as the x-axis). In the same theory level, a one-dimensional periodic boundary condition (PBC) [35] along the CNT axis was employed to calculate the structural derivative and electronic property of the infinite SWCNTs and MWCNTs. The PBC calculation, which can better solve the discrete MO model into continuous bands, usually used to simulate the periodic systems. Here, the calculations of all band gaps were performed for 241 k-points in the Brillouin zone. The density of states (DOS) was calculated by the output coefficient matrix of wave functions and the Gaussian broadening width of DOS is set at 0.30 eV.

To test the suitability of the DFT method and basis sets in our systems, bond length, band angle, total energy, and vibration frequency for C_m ($m = 2, 4, 6, 8$) were calculated and compared with the results of available studies (Table 1). The calculated results of the C_m molecule agree with the corresponding and theoretical experimental data, and the error between them is only approximately 0.12%–0.94% [36–40]. Therefore, the calculated method used in this work is reliable.

3. Results and Discussion

3.1. Structural Derivative of the CNTs. The structural derivative process of the SWCNTs and MWCNTs was explored from the corresponding carbon clusters. The finite SWCNTs and MWCNTs were expressed as $[p, k]$, $[p, k]@[2p, k + 2]$, and $[p, k]@[2p, k + 2]@[2p, k + 4]$, respectively [41], where p is the number of carbon atoms for each layer and k is the number of atomic layers.

First, the structural derivative of the finite SWCNTs was investigated in detail. Figure 1(a) shows the structural derivative processes of $[8, k]$ ($k = 2, 3, 4, \ldots, 11$) finite SWCNTs and the corresponding unit cells of infinite SWCNTs, which also represents other stable structures with different p. Layer-by-layer growth approach can be used in the derivative processes, which were also reported by Gavillet [42] and Kiang [26]. In Figure 1, the structures of all finite SWCNTs with different diameters share the following common characteristics: (1) each C atom has three C neighbors to fully fill a sp^2 type hybridization bond; (2) both ends of the finite SWCNTs were

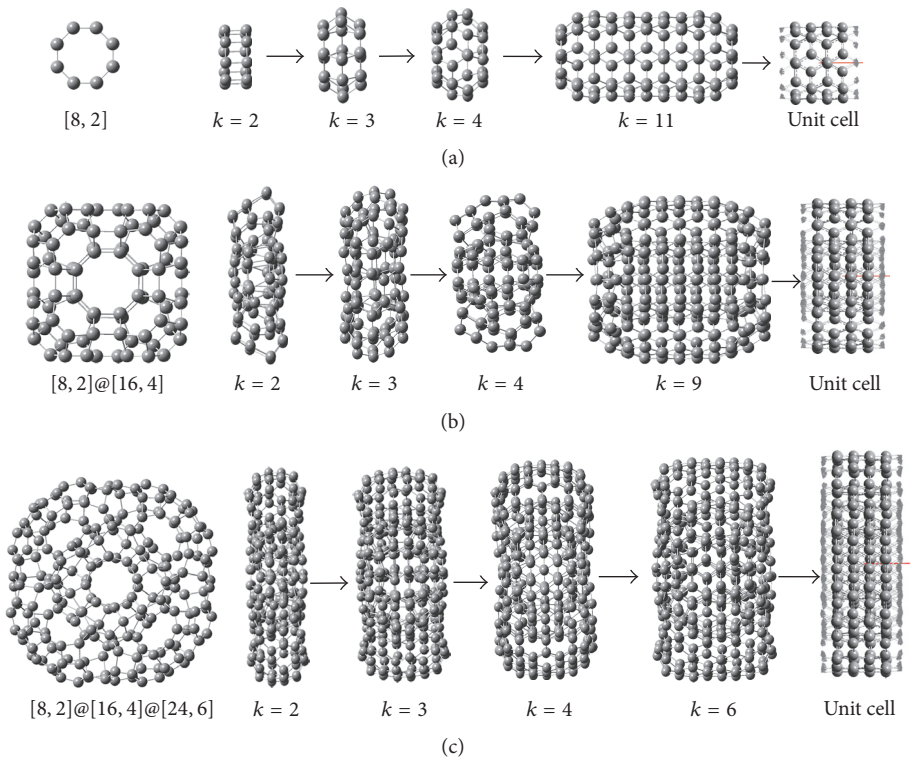

Figure 1: Initial structures, derivative processes of the finite SWCNTs [8, k], DWCNTs [8, k]@[16, $k+2$], and TWCNTs [8, k]@[16, $k+2$]@[24, $k+4$], and the corresponding unit cells of infinite SWCNTs (4, 4), DWCNTs (4, 4)@(8, 8), and TWCNTs (4, 4)@(8, 8)@(12, 12).

formed by four-member-rings (4MRs) and six-member-rings (6MRs). Therefore, p also represents the 4MRs numbers on both ends of the finite SWCNTs.

Furthermore, Figures 1(b) and 1(c) show the structural derivative processes of the finite MWCNTs (including finite DWCNTs [8, k]@[16, k + 2] and TWCNTs [8, k]@[16, k + 2]@[24, $k+4$]) and the corresponding unit cells of the infinite MWCNTs. Here, the stable structures of the finite DWCNTs [p, k]@[2p, $k+2$] and TWCNTs [8, k]@[16, $k+2$]@[24, $k+4$] are obtained by optimized structure and calculated frequency. Here, the stable structures were obtained with no imaginary frequency. The structural derivative processes of the finite MWCNTs are similar to those of finite SWCNTs. However, the initial structure of the finite MWCNTs becomes tire-shape clusters with lip-lip interaction [24] which is consistent with the direct observation in the experiment [25]. Moreover, finite DWCNTs are different from the double-rings of finite SWCNTs. The finite DWCNTs formed by the nesting of two odd SWCNTs show the D_{nh} symmetry in the two ports. The carbon atoms of inner and outer nanotube ports have three nearby neighbor carbon atoms that form the 6MRs and 4MRs. However, one end of finite DWCNTs formed by the nesting of two even SWCNTs is similar to those of two odd SWCNTs but the other end is completely of 6MRs, which showed the symmetry of point group D_{nd}.

Finally, to study the behavior of the structure derivative processes, the changes of the local configurations (including the five-bond lengths and six-bond angles) were monitored along outermost two layers of the finite SWCNTs (Figure 2(a)) and the joint areas of the finite DWCNTs (Figure 2(d)). The structures optimized own diverse C-C bond lengths depending on the special location. For the finite SWCNTs (Figure 2(b)), the bond length values showed that single (1.51 Å) and double bonds (1.34 Å) can be formed along the outermost two layers of the finite SWCNTs during the derivative process. Regarding the finite DWCNTs (Figure 2(e)), the finite DWCNTs may have had diamond-like bonds (1.61 Å) that were formed at both ends. In Figure 2, the changes in bond lengths and bond angles were not stabilized until $k > 4$. Therefore, the carbon clusters first gradually grew longer with a global reconstruction upon $k \leq 4$. Afterwards, it become finite CNTs via layer-by-layer growth with a local reconstruction at the two outermost ends upon $k > 4$. Moreover, the calculated results also demonstrated a universal derivative process for all finite SWCNTs and MWCNTs with different p. Gleaned from the results of the CNT growth processes by Shibuta [43] and Fan et al. [44], the derivative process of the finite CNTs follows the formation mechanism of CNTs in this work.

3.2. Stability and Electronic Property. Based on the structural derivatives of finite SWCNTs and DWCNTs, average cohesive energy (E_b) is calculated to measure the stability of finite CNTs. E_b is defined as the cohesive energy that is related to the assembly of the tubes and the influences of the length

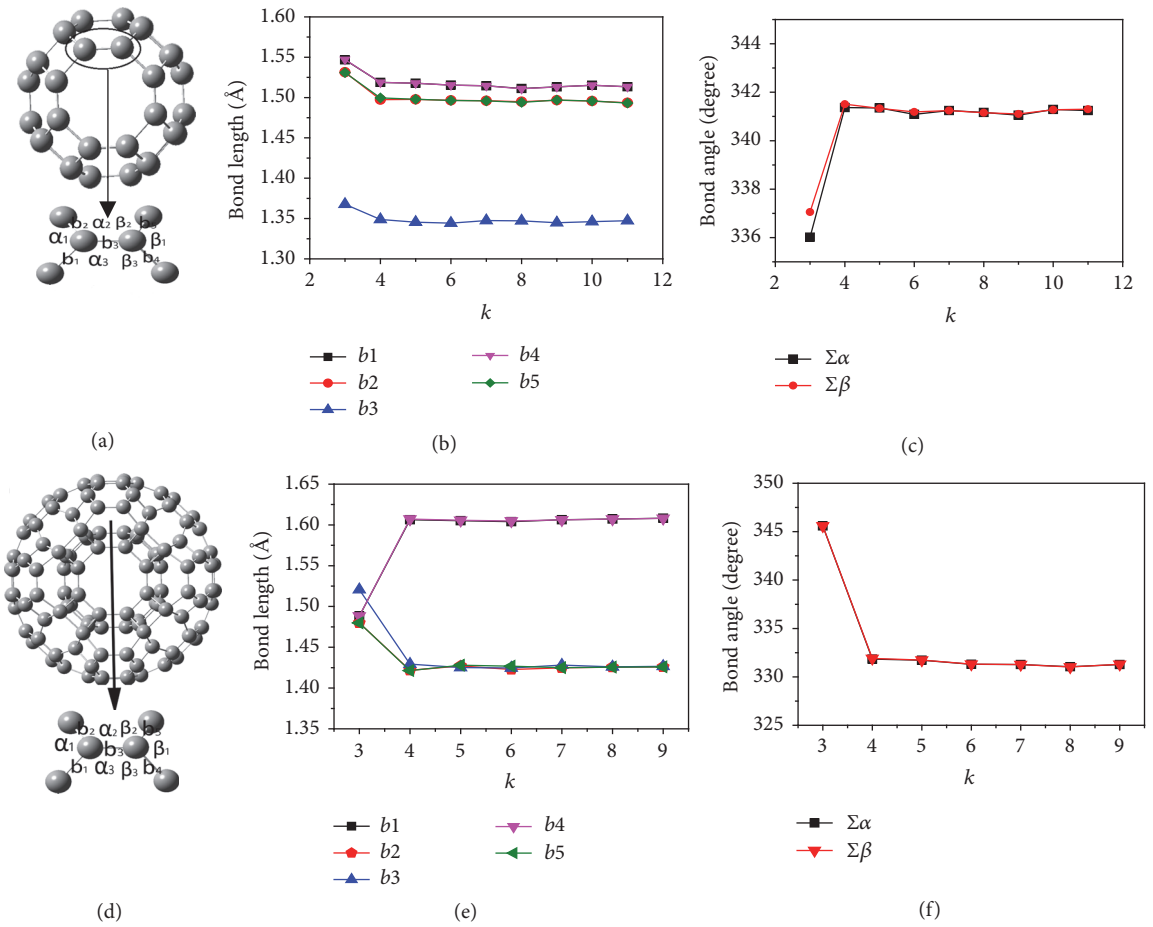

FIGURE 2: Local configurations of the finite SWCNTs [8, k] (a) and DWCNTs [8, k]@[16, $k + 2$] (d); and the changes in bond length (b, e) and bond angle (c, f) versus k.

and diameter. E_b' is the dependence of the reduced interwall cohesive energy for the finite DWCNTs, calculated by

$$E_b(k) = \frac{mE(C) - E(\text{CNTs})}{m} \quad (1)$$

$$E_b'(k) = \frac{[E(\text{CNT})_o + \text{E}(\text{CNT})_i] - E(\text{DWCNT})}{k+2}, \quad (2)$$

where m is the number of carbon atoms in the finite CNTs, $E(C)$ and $E(\text{CNTs})$ represent the total energies of ground state of carbon atoms and finite CNTs for (1), respectively, and $E(\text{CNT})_o$, $E(\text{CNT})_i$, and $E(\text{DWCNT})$ represent total energies of the outermost finite SWCNT [$2p$, $k + 2$], inner finite SWCNT [p, k], and the finite DWCNT [p, k]@[$2p$, $k + 2$] in (2), respectively.

Figures 3(a) and 3(b) show the cohesive energy $E_b(k)$ as a function of length k. For the finite SWCNTs and DWCNTs, $E_b(k)$ increases gradually as k increases following a certain p. However, the increments of cohesive energy of the finite SWCNTs and DWCNTs decrease gradually as k increase, which indicates that finite SWCNTs and DWCNTs increasingly stabilize as the length increases. E_b of the finite CNTs gradually stabilize upon $k > 4$, which is similar to the structural derivative of the finite CNTs depicted earlier. Figure 3(c) shows the change of reduced interwall cohesive energy with increased k upon formation of finite DWCNTs by the corresponding finite SWCNTs. The results showed that E_b' of the reduced interwall cohesive energy is gradually stabilized upon $k > 4$. However, in the shorter interwall distances of the finite DWCNTs, such as [6, k]@[12, $k + 2$] and [8, k]@[16, $k + 2$], E_b' of the finite DWCNTs significantly changed upon increase of k. The result is possibly due to strong interactions among the inner and outer finite SWCNTs with a small distance. Results showed that the finite CNTs may be more stable when they are double-walled or longer.

To examine the above-mentioned results, different diameters of the finite SWCNTs with the same length ($k = 11$) were used. The radial-breathing mode (RBM) frequencies of the finite SWCNTs were measured in the low frequency region of Raman spectroscopy. RBM played a crucial role in determining the diameters of CNTs among the several Raman-active vibration modes of SWCNTs. The relationship between RBM frequency and the inverse of the SWCNTs diameter is nonlinear in the following formula [45]:

$$f_{\text{RMB}}^{*}\left(\text{cm}^{-1}\right) = \frac{238}{d^{0.93}}. \quad (3)$$

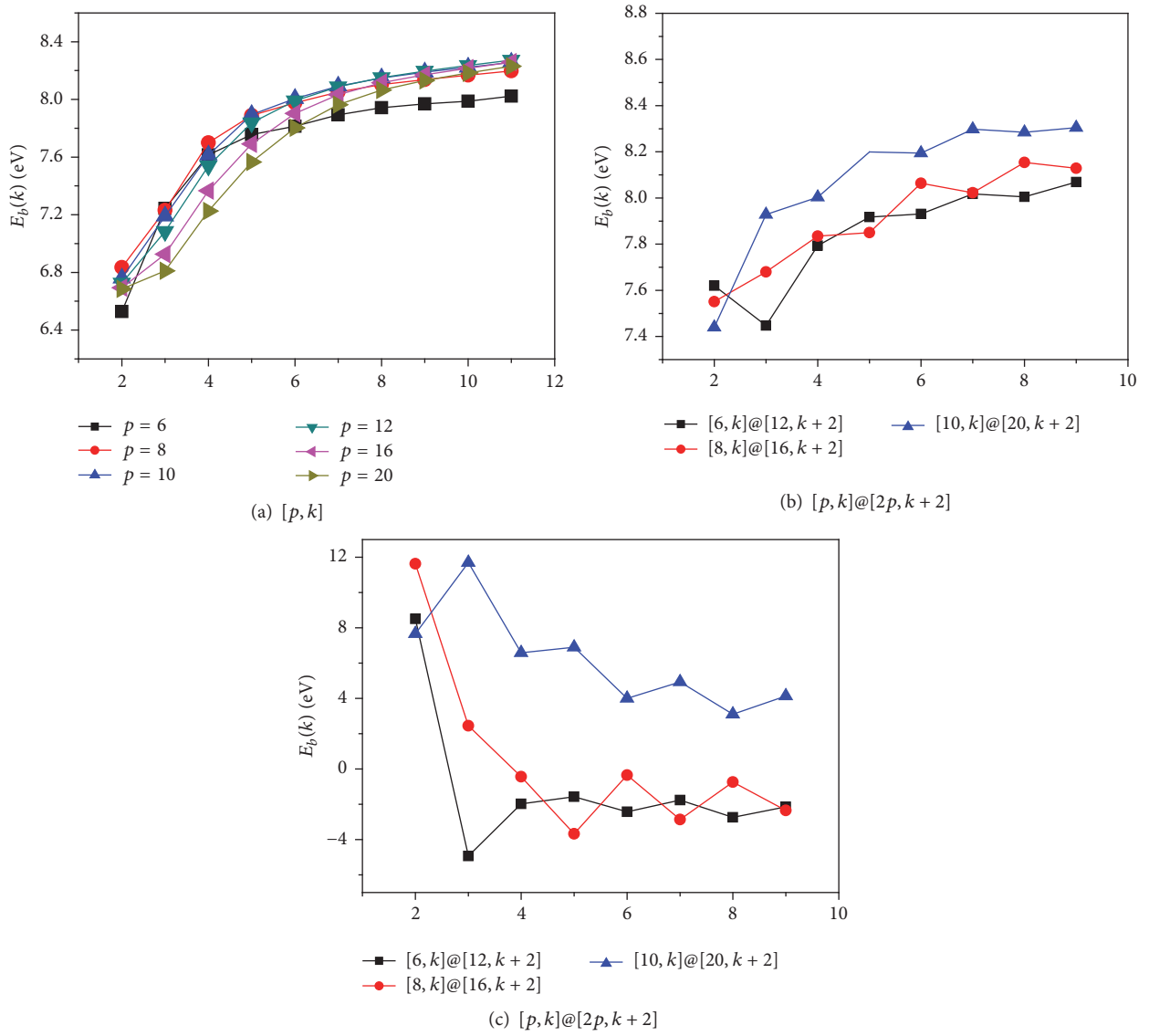

FIGURE 3: (a) Average cohesive energies of finite SWCNTs and (b) DWCNTs and (c) the dependence of the reduced interwall cohesive energy for finite DWCNTs.

Figure 4 shows the relationship between diameters and RBM frequencies of the SWCNTs in the low frequency region. The calculated data can be fitted by the nonlinear formula:

$$f_{\mathrm{RMB}}\left(\mathrm{cm}^{-1}\right) = \frac{238}{d^{0.9222}} + 0.9881. \quad (4)$$

Here, the correlation coefficient is 0.9971 and the standard error is 0.0183. According to the fitting results, the finite SWCNTs gain similar characteristics with SWCNTs upon reaching a certain length.

To study the electronic properties of the finite SWCNTs and MWCNTs, the values of the energy gaps (E_g) and Fermi energy (E_F) were calculated. Figure 5 shows the electronic properties of finite SWCNTs [8, k] and DWCNTs [8, k]@[16, k + 2]. As k increases, the neighboring energy levels of finite CNTs gradually converge and approach the HOMO or LUMO, and E_F of finite CNTs also become relatively stable. The finite SWCNTs [8, k] have a nonzero value for their energy gap HOMO-LUMO, with oscillating dependencies on the length. Here, the changes in electronic properties of finite SWCNTs (5, 5) investigated by Jerzy et al. [46] are similar to our results. However, the energy gaps of the finite DWCNT [8, k]@[16, k + 2] ranges from 2.42 to 0.94 eV, which gradually decreases and stabilizes as k increases. The calculated results show that the electronic property of the finite DWCNTs depending on the length is different from that of the finite SWCNTs, which provides a theoretical guidance for the potential applications of carbon nanodevices (such as supercapacitor and molecular switch).

In addition, the Mulliken charge distribution can be generated for all the finite SWCNTs and DWCNTs. Using the Mulliken charge transfer to investigate the chemical activity of the clusters is simple and efficient [47]. Taking the finite

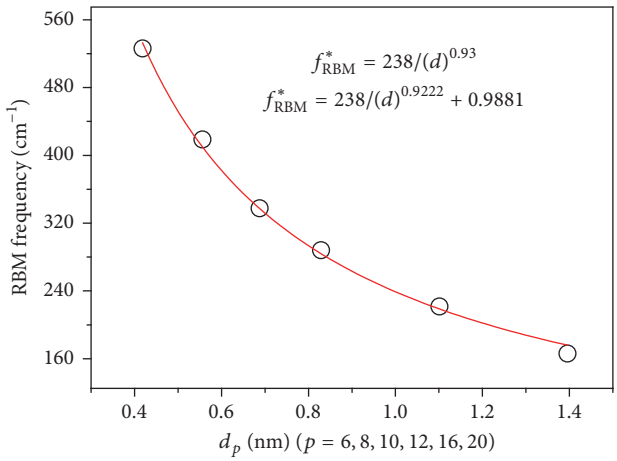

Figure 4: Diameters of finite SWCNTs depending on RBM frequencies for isolated tubes.

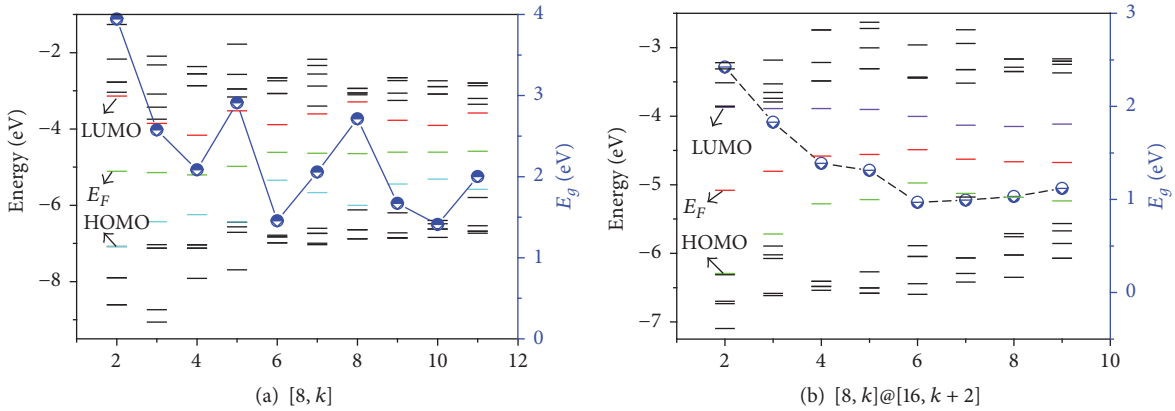

Figure 5: Energy gaps, Fermi energy levels, and energy levels of nearby frontier orbits of the finite SWCNTs [8, k] (a) and finite DWCNTs [8, k]@[16, k + 2] (b).

SWCNTs [10, k] and DWCNTs [10, k]@[20, k + 2] as examples, Figure 6 shows the main Mulliken charge distribution of the finite SWCNTs [10, k] and DWCNTs [10, k]@[20, k + 2] at different lengths (k). The Mulliken charge transfer of the carbon atoms of the finite SWCNTs gradually shifted from the center to both ends of the structure when the length increased. However, the most charges gained or lost of the Mulliken charge distribution were concentrated on both ends of the finite DWCNTs [10, k]@[20, k + 2] as the length increased. Therefore, the results indicated that the chemical activity of the finite SWCNTs and DWCNTs are stronger on both ends, which causes the finite SWCNTs and MWCNTs to become longer and more stable. The chemical activities of the CNTs were applied to catalyst materials, hydrogen storage materials, medical and other aspects.

3.3. Infinite SWCNTs and MWCNTs. As k elongates, the finite CNTs stabilize, which allows us to investigate the stability of the infinite SWCNTs and MWCNTs. Similar to the finite CNTs, the armchair infinite SWCNTs and MWCNTs are represented as (n, n), (n, n)@($2n$, $2n$), and (n, n)@($2n$, $2n$)@($3n$, $3n$), respectively. The repeated unit cells of the SWCNTs and MWCNTs can be formed by removing two parallel polygons at both ends of corresponding finite CNTs (Figure 1).

Figure 7 shows the cohesive energies of infinite SWCNTs and MWCNTs. Compared with the calculated results of the finite CNTs (seen in Figure 3), the cohesive energies of infinite SWCNTs and DWCNTs are slightly larger than the corresponding finite CNTs. For instance, the cohesive energy of finite SWCNTs [8, 11] is 8.19 eV, which is smaller than the 8.45 eV of infinite SWCNT (4, 4). The cohesive energy of the finite DWCNTs [8, 9]@[16, 11] is 8.15 eV, whereas the value of infinite DWCNT (4, 4)@(8, 8) is 8.55 eV. The result indicated that the infinite SWCNTs and DWCNTs are more stable than their corresponding finite SWCNTs and DWCNTs, which illustrate that finite CNTs can be longer. Moreover, the cohesive energy of infinite TWCNTs is slightly higher than that of the DWCNTs with a higher k (Figure 7), which indicates that infinite CNTs become increasingly stable as the

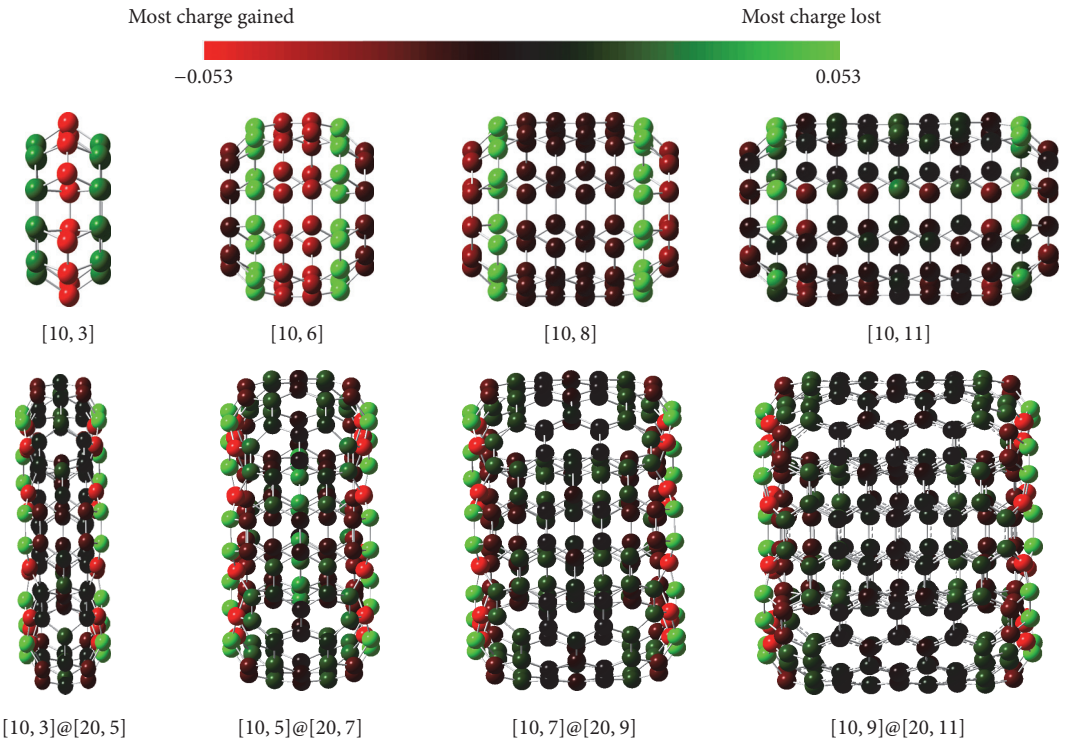

FIGURE 6: Change in the Mulliken charge distributions of the finite SWCNTs [10, k] and DWCNTs [10, k]@[20, k + 2] as k elongates.

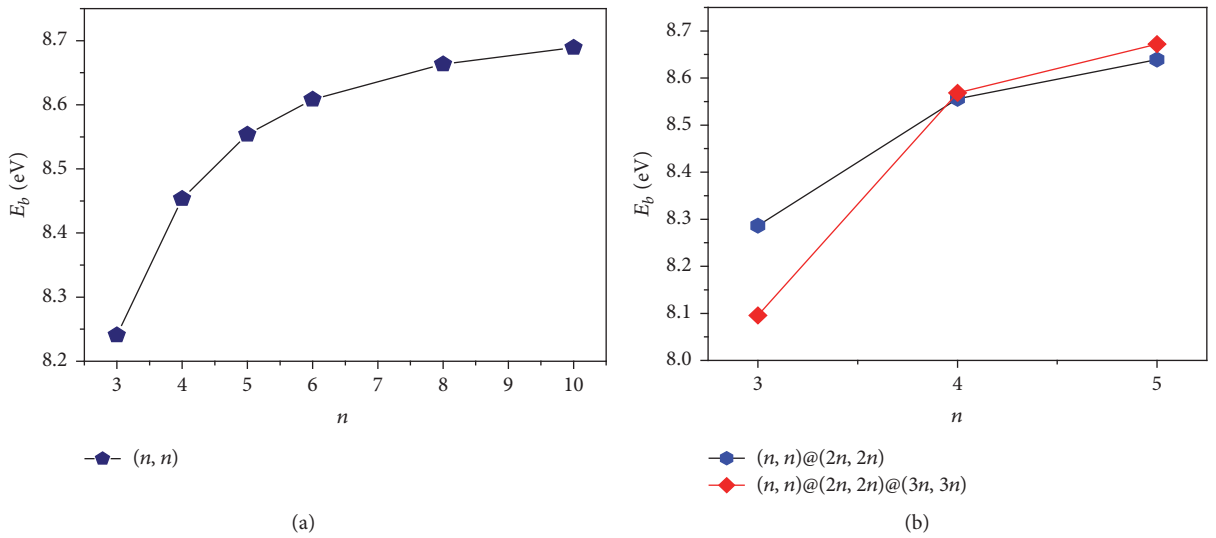

FIGURE 7: Cohesive energies of (n, n) SWCNTs, (n, n)@(2n, 2n) DWCNTs, and (n, n)@(2n, 2n)@(3n, 3n) TWCNTs.

diameter and walls increase. Therefore, the cohesive energies of CNTs can effectively explain why the large diameter and MWCNTs synthesis were easy in experiment [48].

Similar to the HOMO and LUMO of a finite system, the HOCO and LUCO can be defined to study the electronic structures of infinite CNTs. The results of the HOCO and LUCO energies, the indirect gaps, and the minimum direct gaps of all SWCNTs were calculated and are listed in Table 2. The infinite SWCNTs have small band gaps, which are similar in the previous studies [49]. For the DWCNTs, the (3, 3)@(6, 6) DWCNTs illustrates the semiconductor characteristics (Figure 8). The interwall distance of (3, 3)@(6, 6) DWCNTs is small (<0.34 nm) [50], which produces a strong coupling between walls and opens the level of π and π^* overlap [51, 52], resulting in a band gap of 0.699 eV. The band structures of the DWCNTs (4, 4)@(8, 8), (5, 5)@(10, 10), and all TWCNTs present an overlap (Dirac point) between π and π^* level near the Fermi levels, which shows the metallicity [53]. The result illustrated that MWCNTs formed by corresponding metallic SWCNTs retain the unique electronic properties of armchair

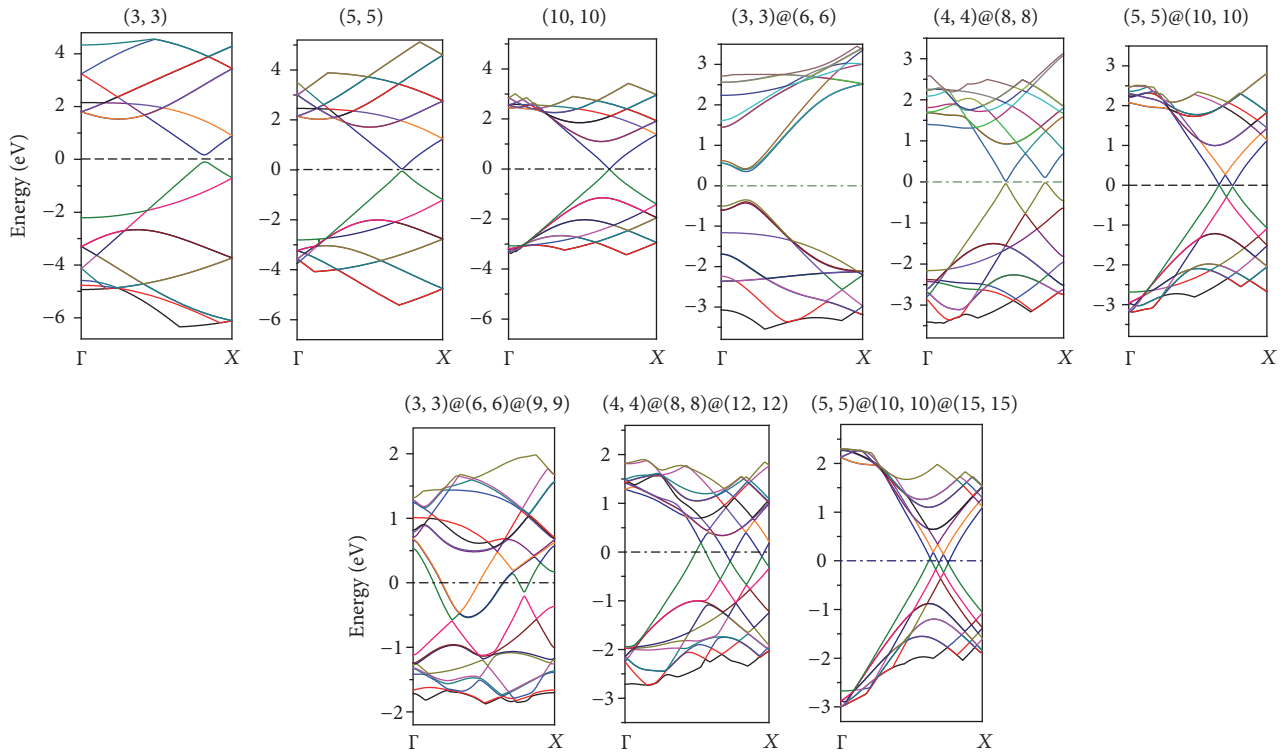

Figure 8: Energy band structures (dispersion along Γ-X direction of the Brillouin zone) of the infinite SWCNTs, DWCNTs, and TWCNTs. The Fermi level is set to zero.

Table 2: Calculated electronic structures for the infinite SWCNTs by B3LYP/3-21G(d) with PBC method.

CNTs	HOCO (eV)	LUCO (eV)	Indirect gap (eV)	Min direct gap (eV)
(3,3)	−4.447	−4.179	0.268	0.268
(4,4)	−4.440	−4.262	0.178	0.178
(5,5)	−4.431	−4.338	0.093	0.093
(6,6)	−4.449	−4.375	0.074	0.074
(8,8)	−4.486	−4.423	0.063	0.063
(10,10)	−4.480	−4.460	0.020	0.020

SWCNTs. The results of band structure of the DWCNT (5, 5)@(10, 10) agreed with the calculation obtained by Kwon and Tománek [54]. However, the band structure of MWCNTs was not simply constituted by that of the corresponding SWCNTs due to the interaction between the interwalls which destroys the symmetry of the system and results in a split of degenerate energy bands. The band structure of MWCNTs is very different to that of SWCNTs (Figure 8), which is mainly caused by the coupling effect of MWCNTs between interwalls.

To further study the band structure of the CNTs, the total density of states (TDOS) and the partial density of states (PDOS) of the CNTs were studied. Figure 9 displays the TDOS and PDOS of the (4, 4), (8, 8) SWCNTs, (4, 4)@(8, 8) DWCNTs, and (4, 4)@(8, 8)@(12, 12) TWCNTs near the Fermi level which were formed by the DOS of orbits of carbon atoms on the walls of CNTs. The walls of CNTs are very similar to those of graphene in which the π bond is formed by the atomic orbit of p_z of graphite layer placed in the X-Y plane. Due to the curled wall of CNTs, the stretch direction of p_z orbit of the carbon atoms on the different positions of tube walls was no longer fixed on the z-axis but along the radius r of tubes [55, 56]. Therefore, the atomic orbit of p_z may be combined by one or several atomic orbits of $2p_x$, $2p_y$, and $2p_z$. From Figure 9, we can conclude the following:

(1) The distributions of the TDOS between the smaller and larger diameters of CNTs are not significantly different near the Fermi level, such as the diameter of 5.54 and 10.94 Å for the SWCNTs (4, 4) and (8, 8), respectively.

(2) For the distribution of the TDOS, the SWCNTs (n, n) are similar to that of MWCNTs (n, n)@($2n$, $2n$) and (n, n)@($2n$, $2n$)@($3n$, $3n$) near the Fermi level. Therefore, the type of CNTs has little effect on the composition of the energy band near the Fermi level.

(3) The PDOS of 2 s orbits have little distribution near the Fermi level, which indicates that the energy band near the Fermi level does not contain the 2 s orbital elements. The reasons are that the σ bonds are mainly involved in the 2 s orbits and that the energy distribution of the bonds is $\sigma < \pi < \pi^* < \sigma^*$, in general [57]. Therefore, the distribution of the PDOS of 2 s orbits is very little near the Fermi level because

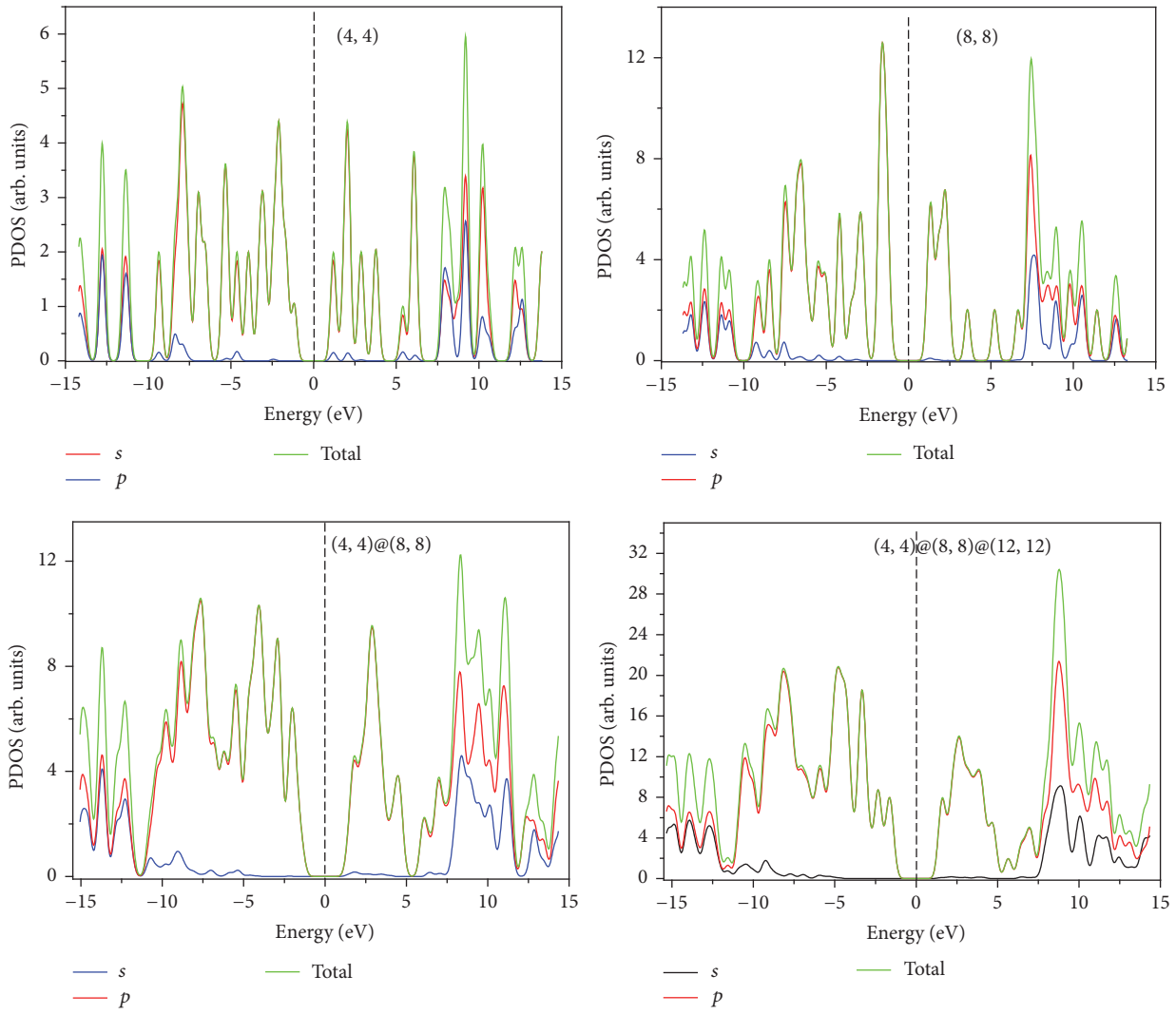

Figure 9: TDOS and PDOS of the SWCNTs (4, 4), (8, 8), DWCNTs (4, 4)@(8, 8), and TWCNTs (4, 4)@(8, 8)@(12, 12). The Fermi level is set to zero.

the main distribution of 2 s orbits is in the region of low energy.

The analysis of the PDOS pointed out that the diameters and walls of CNTs had no obvious effect on the distribution of TDOS near the Fermi of the SWCNTs and MWCNTs. The main component of π bond was formed by the p orbits, which were concentrated in the vicinity of the Fermi level, including all $2p$ orbits of carbon atoms. Therefore, the results can provide an effective support for the application of CNTs on physical (such as conductivity, semiconductor, and superconductivity) [58–60] and chemical properties (stability, adsorption, and catalysis reactivity) [61, 62].

4. Conclusions

The structural derivative and electronic property of armchair CNTs were studied using DFT calculation. We began the investigation by trying to explore the structural derivatives of the armchair SWCNTs and MWCNTs from carbon clusters. Notably, the results of the initial structures of the CNT were determined from carbon clusters. The structural derivative processes demonstrated that the armchair SWCNTs and MWCNTs were obtained through layer-by-layer growth. For the structural derivative processes, the carbon clusters first increasingly elongate with a global reconstruction; then, it becomes finite CNTs using the layer-by-layer growth with a local reconstruction at the two outermost ends; finally, the infinite CNTs can be obtained by the unit cells that were determined by the periodic characteristics based on finite CNTs. The results of the cohesive energies explain successful obtainment of the long and stable CNTs. From the results of band structure, all of SWCNTs have small direct band gaps. However, the band structures of the infinite MWCNTs were different from those of the infinite SWCNTs. The DWCNTs (3, 3)@(6, 6) show a strong semiconductor characteristic. The band structures of the DWCNTs (4, 4)@(8, 8), (5, 5)@(10, 10), and all TWCNTs show metallicity. The result

illustrated that the MWCNTs formed by the corresponding metallic SWCNTs retain the unique electronic properties of armchair SWCNTs. The analysis of the PDOS showed that the diameters and walls of CNTs had no significant effect on the distribution of DOS near the Fermi of the SWCNTs and MWCNTs. Finally, we hope this work will provide insight into the comprehension of growth process of armchair CNTs.

Competing Interests

The authors declare that they have no competing interests.

Acknowledgments

The authors acknowledge the financial support by NSFC (11464044), Scientific Research Program for Graduate Students of Xinjiang Uygur Autonomous Region (XJGRI2015108), and Key Laboratory of Mineral Luminescence Materials and Microstructures at University of Education Department of Xinjiang Uygur Autonomous Region of China (WDXY1506 and WDXY1505).

References

[1] D. Jariwala, V. K. Sangwan, L. J. Lauhon, T. J. Marks, and M. C. Hersam, "Carbon nanomaterials for electronics, optoelectronics, photovoltaics, and sensing," *Chemical Society Reviews*, vol. 42, no. 7, pp. 2824–2860, 2013.

[2] A. Manzano-Ramírez, A. Moreno-Bárcenas, M. Apatiga-Castro, E. M. Rivera-Muñoz, R. Nava-Mendoza, and R. Velázquez-Castillo, "An overview of carbon nanotubes: synthesis, purification and characterization," *Current Organic Chemistry*, vol. 17, no. 17, pp. 1858–1866, 2013.

[3] S. Iijima, "Helical microtubules of graphitic carbon," *Nature*, vol. 354, no. 6348, pp. 56–58, 1991.

[4] L.-M. Peng, Z. Zhang, and S. Wang, "Carbon nanotube electronics: recent advances," *Materials Today*, vol. 17, no. 9, pp. 433–442, 2014.

[5] V. N. Popov, "Carbon nanotubes: properties and application," *Materials Science and Engineering R: Reports*, vol. 43, no. 3, pp. 61–102, 2004.

[6] P. M. Ajayan, "Nanotubes from carbon," *Chemical Reviews*, vol. 99, pp. 1787–1800, 1999.

[7] M. F. L. De Volder, S. H. Tawfick, R. H. Baughman, and A. J. Hart, "Carbon nanotubes: present and future commercial applications," *Science*, vol. 339, no. 6119, pp. 535–539, 2013.

[8] F. Yang, X. Wang, D. Zhang et al., "Chirality-specific growth of single-walled carbon nanotubes on solid alloy catalysts," *Nature*, vol. 510, no. 7506, pp. 522–524, 2014.

[9] F. Ding, J. Y. Huang, and B. I. Yakobson, "Comment on 'mechanism for superelongation of carbon nanotubes at high temperatures'," *Physical Review Letters*, vol. 103, no. 3, Article ID 039601, 2009.

[10] F. Ding, A. R. Harutyunyan, and B. I. Yakobson, "Dislocation theory of chirality-controlled nanotube growth," *Proceedings of the National Academy of Sciences of the United States of America*, vol. 106, no. 8, pp. 2506–2509, 2009.

[11] M. Marchand, C. Journet, D. Guillot, J.-M. Benoit, B. I. Yakobson, and S. T. Purcell, "Growing a carbon nanotube atom by atom: 'and yet it does turn'," *Nano Letters*, vol. 9, no. 8, pp. 2961–2966, 2009.

[12] S. Iijima and T. Ichihashi, "Single-shell carbon nanotubes of 1-nm diameter," *Nature*, vol. 363, no. 6430, pp. 603–605, 1993.

[13] D. S. Bethune, C. H. Kiang, M. S. de Vries et al., "Cobalt-catalysed growth of carbon nanotubes with single-atomic-layer walls," *Nature*, vol. 363, no. 6430, pp. 605–607, 1993.

[14] T. Guo, P. Nikolaev, A. G. Rinzler, D. Tomanek, D. T. Colbert, and R. E. Smalley, "Self-assembly of tubular fullerenes," *The Journal of Physical Chemistry*, vol. 99, no. 27, pp. 10694–10697, 1995.

[15] A. Thess, R. Lee, P. Nikolaev et al., "Crystalline ropes of metallic carbon nanotubes," *Science*, vol. 273, no. 5274, pp. 483–487, 1996.

[16] N. Hatta and K. Murata, "Very long graphitic nano-tubules synthesized by plasma-decomposition of benzene," *Chemical Physics Letters*, vol. 217, no. 4, pp. 393–402, 1994.

[17] H. Dai, A. G. Rinzler, P. Nikolaev, A. Thess, D. T. Colbert, and R. E. Smalley, "Single-wall nanotubes produced by metal-catalyzed disproportionation of carbon monoxide," *Chemical Physics Letters*, vol. 260, no. 3-4, pp. 471–475, 1996.

[18] W. Z. Li, S. S. Xie, L. X. Qian et al., "Large-scale synthesis of aligned carbon nanotubes," *Science*, vol. 274, no. 5293, pp. 1701–1703, 1996.

[19] S. Arepalli and C. D. Scott, "Spectral measurements in production of single-wall carbon nanotubes by laser ablation," *Chemical Physics Letters*, vol. 302, no. 1-2, pp. 139–145, 1999.

[20] F. Ding, K. Bolton, and A. Rosén, "Nucleation and growth of single-walled carbon nanotubes: a molecular dynamics study," *Journal of Physical Chemistry B*, vol. 108, no. 45, pp. 17369–17377, 2004.

[21] W.-Q. Deng, X. Xu, and W. A. Goddard III, "A two-stage mechanism of bimetallic catalyzed growth of single-walled carbon nanotubes," *Nano Letters*, vol. 4, no. 12, pp. 2331–2335, 2004.

[22] Y. Tian, Z. Hu, Y. Yang et al., "In situ TA-MS study of the six-membered-ring-based growth of carbon nanotubes with benzene precursor," *Journal of the American Chemical Society*, vol. 126, no. 4, pp. 1180–1183, 2004.

[23] S. Iijima, P. M. Ajayan, and T. Ichihashi, "Growth model for carbon nanotubes," *Physical Review Letters*, vol. 69, no. 21, pp. 3100–3103, 1992.

[24] M. B. Nardelli, C. Brabec, A. Maiti, C. Roland, and J. Bernholc, "Lip-lip interactions and the growth of multiwalled carbon nanotubes," *Physical Review Letters*, vol. 80, no. 2, pp. 313–316, 1998.

[25] C. Jin, K. Suenaga, and S. Iijima, "Direct evidence for lip-lip interactions in multi-walled carbon nanotubes," *Nano Research*, vol. 1, no. 5, pp. 434–439, 2008.

[26] C.-H. Kiang, "Carbon rings and cages in the growth of single-walled carbon nanotubes," *The Journal of Chemical Physics*, vol. 113, no. 11, pp. 4763–4766, 2000.

[27] M. Lin, J. P. Tan, C. Boothroyd, K. P. Loh, E. S. Tok, and Y. L. Foo, "Direct observation of single-walled carbon nanotube growth at the atomistic scale," *Nano Letters*, vol. 6, no. 3, pp. 449–452, 2006.

[28] J. Y. Raty, F. Gygi, and G. Galli, "Growth of carbon nanotubes on metal nanoparticles: a microscopic mechanism from ab initio molecular dynamics simulations," *Physical Review Letters*, vol. 142, p. 95, 2005.

[29] M. J. Frisch, G. W. Trucks, H. B. Schlegel et al., *Gaussian 03, Revision E01*, Gaussian, Wallingford, Conn, USA, 2004.

[30] C. Lee, W. Yang, and R. G. Parr, "Development of the Colle-Salvetti correlation-energy formula into a functional of the electron density," *Physical Review B*, vol. 37, no. 2, pp. 785–789, 1988.

[31] A. D. Becke, "Density-functional thermochemistry. III. The role of exact exchange," *Journal of Chemical Physics*, vol. 98, no. 7, pp. 5648–5652, 1993.

[32] X. Lu, Z. Chen, and P. V. R. Schleyer, "Are stone-wales defect sites always more reactive than perfect sites in the sidewalls of single-wall carbon nanotubes?" *Journal of the American Chemical Society*, vol. 127, no. 1, pp. 20–21, 2005.

[33] F. Ding, "Theoretical study of the stability of defects in single-walled carbon nanotubes as a function of their distance from the nanotube end," *Physical Review B*, vol. 72, no. 24, Article ID 245409, 2005.

[34] J. M. L. Martin, J. El-Yazal, and J.-P. François, "Basis set convergence and performance of density functional theory including exact exchange contributions for geometries and harmonic frequencies," *Molecular Physics*, vol. 86, no. 6, pp. 1437–1450, 1995.

[35] J. P. Perdew, K. Burke, and M. Ernzerhof, "Generalized gradient approximation made simple," *Physical Review Letters*, vol. 77, no. 18, pp. 3865–3868, 1996.

[36] J. Hutter, H. P. Luethi, and F. J. Diederich, "Structures and vibrational frequencies of the carbon molecules C2-C18 calculated by density functional theory," *Journal of the American Chemical Society*, vol. 116, no. 2, pp. 750–756, 1994.

[37] K. P. Huber and G. Herzberg, *Molecular Spectra and Molecular Structure IV. Constants of Diatomic Molecules*, Van Nostrand Reinhold, New York, NY, USA, 1979.

[38] J. M. L. Martin, J. El-Yazal, and J. P. Francois, "Structure and vibrational spectra of carbon clusters C_n(n = 2–10, 12, 14, 16, 18) using density functional theory including exact exchange contributions," *Chemical Physics Letters*, vol. 242, no. 6, pp. 570–579, 1995.

[39] K. Raghavachari and J. S. Binkley, "Structure, stability, and fragmentation of small carbon clusters," *The Journal of Chemical Physics*, vol. 87, no. 4, pp. 2191–2197, 1987.

[40] K. Raghavachari, R. A. Whiteside, and J. A. Pople, "Structures of small carbon clusters: cyclic ground state of C6," *The Journal of Chemical Physics*, vol. 85, no. 11, pp. 6623–6628, 1986.

[41] C. Yao, Y. Tang, D. Liu, and H. Zhu, "The structure evolution process and the electronic properties of armchair boron nitride nanotubes," *Superlattices and Microstructures*, vol. 92, pp. 198–209, 2016.

[42] J. Gavillet, A. Loiseau, C. Journet, F. Willaime, F. Ducastelle, and J.-C. Charlier, "Root-growth mechanism for single-wall carbon nanotubes," *Physical Review Letters*, vol. 87, no. 27, Article ID 275504, 2001.

[43] Y. Shibuta, "A numerical approach to the metal-catalyzed growth process of carbon nanotubes," *Diamond and Related Materials*, vol. 20, no. 3, pp. 334–338, 2011.

[44] S. Fan, L. Liu, and M. Liu, "Monitoring the growth of carbon nanotubes by carbon isotope labelling," *Nanotechnology*, vol. 14, no. 10, pp. 1118–1123, 2003.

[45] S. Rols, A. Righi, L. Alvarez et al., "Diameter distribution of single wall carbon nanotubes in nanobundles," *European Physical Journal B*, vol. 18, no. 2, pp. 201–205, 2000.

[46] C. Jerzy, R. Niny, and M. David, "Electronic structures and energetics of [5, 5] and [9, 0] single-walled carbon nanotubes," *Journal of the American Chemical Society*, vol. 8485, p. 124, 2002.

[47] S. Nagakura, "Mulliken's charge-transfer theory and its application to chemical reactions," *Molecular Crystals and Liquid Crystals*, vol. 126, no. 1, pp. 9–18, 1985.

[48] C. Journet, M. Picher, and V. Jourdain, "Carbon nanotube synthesis: from large-scale production to atom-by-atom growth," *Nanotechnology*, vol. 23, pp. 142001–142019, 2012.

[49] H.-W. Wang, B.-C. Wang, W.-H. Chen, and M. Hayashi, "Localized Gaussian type orbital-periodic boundary condition-density functional theory study of infinite-length single-walled carbon nanotubes with various tubular diameters," *Journal of Physical Chemistry A*, vol. 112, no. 8, pp. 1783–1790, 2008.

[50] J.-C. Charlier and J.-P. Michenaud, "Energetics of multilayered carbon tubules," *Physical Review Letters*, vol. 70, no. 12, p. 1858, 1993.

[51] R. Moradian, S. Azadi, and H. Refii-Tabar, "When double-wall carbon nanotubes can become metallic or semiconducting," *Journal of Physics Condensed Matter*, vol. 19, no. 17, Article ID 176209, 2007.

[52] M. Pudlak and R. Pincak, "Electronic properties of double-layer carbon nanotubes," *The European Physical Journal B*, vol. 67, no. 4, pp. 565–576, 2009.

[53] Y. L. Chen, B. Liu, K. C. Hwang, and Y. Huang, "A theoretical evaluation of load transfer in multi-walled carbon nanotubes," *Carbon*, vol. 49, no. 1, pp. 193–197, 2011.

[54] Y.-K. Kwon and D. Tománek, "Electronic and structural properties of multiwall carbon nanotubes," *Physical Review B*, vol. 58, no. 24, pp. R16001–R16004, 1998.

[55] I. Suarez-Martinez, P. J. Higginbottom, and N. A. Marks, "Molecular dynamics simulations of the transformation of carbon peapods into double-walled carbon nanotubes," *Carbon*, vol. 48, no. 12, pp. 3592–3598, 2010.

[56] C. Shen, A. H. Brozena, and Y. Wang, "Double-walled carbon nanotubes: challenges and opportunities," *Nanoscale*, vol. 3, no. 2, pp. 503–518, 2011.

[57] R. Hoffmann, "A chemical and theoretical way to look at bonding on surfaces," *Reviews of Modern Physics*, vol. 60, no. 3, pp. 601–628, 1988.

[58] R. Krupke, F. Hennrich, H. von Löhneysen, and M. M. Kappes, "Separation of metallic from semiconducting single-walled carbon nanotubes," *Science*, vol. 301, no. 5631, pp. 344–347, 2003.

[59] E. Joselevich and C. M. Lieber, "Vectorial growth of metallic and semiconducting single-wall carbon nanotubes," *Nano Letters*, vol. 2, no. 10, pp. 1137–1141, 2002.

[60] D. Chattopadhyay, I. Galeska, and F. Papadimitrakopoulos, "A route for bulk separation of semiconducting from metallic single-wall carbon nanotubes," *Journal of the American Chemical Society*, vol. 125, no. 11, pp. 3370–3375, 2003.

[61] S. Niyogi, M. A. Hamon, H. Hu et al., "Chemistry of single-walled carbon nanotubes," *Accounts of Chemical Research*, vol. 35, no. 12, pp. 1105–1113, 2002.

[62] E. Joselevich, "Electronic structure and chemical reactivity of carbon nanotubes: a Chemist's view," *ChemPhysChem*, vol. 5, no. 5, pp. 619–624, 2004.